



## Computational approaches for analyzing fractional impulsive systems in differential equations

Zahra Sharifi<sup>1</sup>, Behrouz Parsa Moghaddam<sup>1,\*</sup>, and Mousa Ilie<sup>2</sup>

<sup>1</sup>Department of Mathematics, Lahijan Branch, Islamic Azad University, Lahijan, Iran.

<sup>2</sup>Department of Mathematics, Rasht Branch, Islamic Azad University, Rasht, Iran.

### Abstract

This research introduces an algorithmically efficient framework for analyzing the fractional impulsive system, which can be seen as specific instances of the broader fractional Lorenz impulsive system. Notably, these systems find pertinent applications within the financial domain. To this end, the utilization of cubic splines is embraced to effectively approximate the fractional integral within the context of the system. The outcomes derived from this method are subsequently compared with those yielded by alternative techniques documented in existing literature, all pertaining to the integration of functions.

Furthermore, the proposed methodology is not only applied to the resolution of the fractional impulsive system, but also extended to encompass scenarios involving the fractional Lorenz system with impulsive characteristics. The discernible effects stemming from the selection of disparate impulse patterns are meticulously demonstrated. In synthesis, this paper endeavors to present a pragmatic and proficient resolution to the intricate challenges posed by impulsive systems.

**Keywords.** Fractional calculus, Fractional dynamical system, Fractional Lorenz impulsive system, Cubic spline.

**1991 Mathematics Subject Classification.** 26A33, 41A15, 49N25, 93C27, 41A05, 65L05.

### 1. INTRODUCTION

Despite fractional calculus roots stretching back over three centuries, the field of fractional calculus has experienced a surge in relevance and applicability, particularly in recent decades. This heightened interest stems from its widespread applications across an array of disciplines. Recent research has demonstrated the effectiveness of fractional differential equations in modeling various real-world phenomena, thereby facilitating advancements in solving complex problems within these domains. Notable contributions in this area include works in physics [13], engineering [45], mechanics [9], chemistry [2], finance [40], and other interdisciplinary applications [3, 14, 27]. These works collectively contribute to the ongoing development and understanding of fractional differential equations across diverse fields.

The impulsive phenomenon manifests across various evolutionary processes of dynamic systems, spanning disciplines such as macroeconomics [17], physics [20], and ecology [25]. It is evident that impulsivity can arise from intricate influences on dynamic systems, encompassing disturbances that impact stability and destabilize oscillations or chaotic systems. Conversely, impulses serve as control forces, intervening when the primary component becomes unstable. Analyzing real-world phenomena with short-term disturbances is facilitated with impulsive systems, highlighting their ability to effectively compensate for process deviations [32]. This underscores the control potential inherent in impulsive perturbations, enabling the manipulation of system behavior. Several rules governing impulse control are outlined in [42, 43].

Impulse differential equations (IDEs) find application in mathematically simulating processes subject to impulsive events throughout their evolution. These equations are extensively studied in systems experiencing short-lived disturbances [44]. Such phenomena are prevalent across various scientific and technological domains, including biocontrol [8], chemostat systems [21], and population dynamics [41]. The existence and uniqueness of IDEs have been investigated

Received: 27 April 2024 ; Accepted: 25 June 2024.

\* Corresponding author. Email: bparsa@iau.ac.ir .

in previous works such as [33, 47, 50]. Furthermore, both analytical and numerical solutions for these equations have been explored in the literature, as evidenced by studies such as [26, 37].

The study of fractional impulsive differential equation (FIDE) as a new branch in mathematics based on fractional calculus has attracted the attention of many researchers [48]. In the last few years, many applications of the fractional calculus of incorrect and arbitrary degrees have been presented, which, along with the development of numerical methods, has promoted the position of this branch of mathematics in other sciences such as control [18], mechanics [36], stock market [30], electronic [16], biology [15, 28]. Recently, FIDEs have been surveyed in the simulation of many problems, including chaotic and super-chaotic devices [51], control [12], and neural networks [7]. In [10], the topological degree approach was used to study the existence of solutions of FIDE. Moreover, the stability of these equations was proposed in [38]. Moreover, the investigation of solutions for these equations was conducted employing a global bifurcation approach in a study by Guan et al. [23]. Zhao et al. [52] examined FIDEs involving non-momentum impulses through a variation method. Odibat et al. [34] utilized the differential transform approach to simulate FIDEs. Kumar et al. [19] proposed a numerical scheme to assess the controllability of FIDEs. Additionally, Parsa-Moghaddam et al. [35] discussed the use of Hermite interpolation for solving FIDEs, while Moniri [29] explored B-spline interpolation for the same purpose.

In this paper, we present a general chaotic system described by a FIDE:

$$\begin{cases} {}^C \mathcal{D}_{0,t}^\varrho x(t) = \Psi(t, x(t)), & \text{for } t \in \Phi' := \Phi \setminus \{t_1, t_2, \dots, t_u\}, \\ \Delta x(t) = x(t_\nu^+) - x(t_\nu) = \Upsilon_\nu(x(t_\nu)), & \text{for } \nu = 1, 2, \dots, u, \\ x(0^+) = x_0, \end{cases} \tag{1.1}$$

where  $\Phi := [0, T]$ ,  $0 < \varrho < 1$ , and the function  $\Psi : \Phi \times \mathbb{R}^n \rightarrow \mathbb{R}^n$  is jointly continuous. The impulsive control law for system (1.1) is represented by a sequence,  $\{t_\nu, \Upsilon_\nu(x(t_\nu))\}$ , which induces sudden changes in the system's state at the instants  $t_\nu$ , where  $t_1 < t_2 < \dots < t_\nu < \dots, \lim_{\nu \rightarrow \infty} t_\nu = T$ , and  $t_1 > t_0 = 0$ . This can be expressed as:

$$\Delta x(t_\nu) = x(t_\nu^+) - x(t_\nu) = \Upsilon_\nu(x(t_\nu)), \tag{1.2}$$

where  $x(t_\nu^+) = \lim_{t \rightarrow t_\nu^+} x(t)$  and  $x(t_\nu) = \lim_{t \rightarrow t_\nu^-} x(t)$ . Here,  $\nu = \lfloor \frac{T}{\omega} \rfloor$ , with  $\omega = t_{\nu+1} - t_\nu < \infty$ . For simplicity, we assume  $x(t_\nu^-) = x(t_\nu)$ . Additionally,  $\Upsilon_\nu(x(t_\nu))$  can be expressed as  $C_\nu x(t_\nu)$ , where  $C_\nu$  are  $n \times n$  matrices.

Additionally, we utilize the Caputo fractional derivative [5, 6], expressed as:

$${}^C \mathcal{D}_{0,t}^\varrho x(t) = \int_0^t \frac{1}{\Gamma(q-\varrho)} (t-\varsigma)^{q-\varrho-1} \cdot x^{(q)}(\varsigma) d\varsigma, \quad 0 \leq q-1 < \varrho \leq q \in \mathbb{N}, \tag{1.3}$$

where  $x(t)$ , the unknown function, is assumed to be continuously differentiable up to  $(q-1)$  times.

The structure of the rest of the paper is outlined in the subsequent sections: Section 2 introduces a proficient method grounded in finite differences for discretizing the FIDE (1.1). The effectiveness and precision of this method are assessed through numerous examples in section 3. Moreover, section 3 delves into the impact of impulses on the chaotic financial impulsive system within the fractional context. Finally, section 4 offers concluding remarks summarizing the findings and insights obtained from this study.

## 2. THEORETICAL RESULTS

In this section, we aim to achieve two primary objectives. Initially, we present an approximation technique for the fractional-order integral. Subsequently, we employ the Proposed Approach to address FIDEs (1.1). To facilitate this, we adopt  $t_m = m\delta$ , where  $m = \{0, 1, \dots, r\}$ , and  $\delta = \frac{T}{r}$  denotes the uniform step size, with  $r \in \mathbb{N}$ . Additionally, we delve into the left Riemann-Liouville fractional integral of order  $\varrho$  ([39]), which is defined as follows:

$$\mathcal{J}_{0,t}^\varrho x(t) = \frac{1}{\Gamma(\varrho)} \int_0^t (t-\varsigma)^{\varrho-1} \cdot x(\varsigma) d\varsigma, \tag{2.1}$$



where  $t, \varrho, \varsigma \in \mathbb{R}^+$  and  $\Gamma(\cdot)$  refers to the Gamma function. To discretize the process, we need to approximate

$$\begin{aligned} \mathcal{J}_{0,t_r}^\varrho x(t) &= \frac{1}{\Gamma(\varrho)} \int_0^{t_r} (t_r - \varsigma)^{\varrho-1} \cdot x(\varsigma) d\varsigma \\ &= \frac{1}{\Gamma(\varrho)} \sum_{m=0}^{r-1} \int_{t_m}^{t_{m+1}} (t_r - \varsigma)^{\varrho-1} x(\varsigma) d\varsigma. \end{aligned}$$

Hence, using cubic spline interpolation will get

$$\mathcal{J}_{0,t_r}^\varrho x(t) \approx \sum_{m=0}^r \frac{\delta^\varrho}{\Gamma(\varrho + 4)} \left( \alpha_{m,r} x_m + \delta \beta_{m,r} x'_m \right), \tag{2.2}$$

where

$$\alpha_{m,r} = \begin{cases} -6(2r + 1 + \varrho)(r - 1)^{\varrho+2} + \left( -6(\varrho + 3)r^2 + 12r^3 + \varrho^3 + 6\varrho^2 + 11\varrho + 6 \right) r^\varrho, & m = 0, \\ 6 \left( (r - m - 1)^{\varrho+2} (2m - 2r - \varrho - 1) + (r - m + 1)^{\varrho+2} (2m - 2r - \varrho + 1 + 4(r - l)^{\varrho+3}) \right), & 1 \leq m < r, \\ 6\varrho + 6, & m = r, \end{cases} \tag{2.3}$$

and

$$\beta_{m,r} = \begin{cases} -(6r + 2\varrho)(r - 1)^{\varrho+2} + \left( \varrho^2 + (5 - 4r)\varrho + 6(r - 1) \right) r^{\varrho+1}, & m = 0, \\ 2(3m - 3r - \varrho)(r - m - 1)^{\varrho+2} - 2(3m - 3r + \varrho)(r - m + 1)^{\varrho+2} - 8(r - m)^{\varrho+2}(\varrho + 3), & 1 \leq m < r, \\ -2\varrho, & m = r. \end{cases} \tag{2.4}$$

**Proposition 2.1.** Consider a function  $x(t)$  belonging to the class  $C^4(\Phi)$ , where  $\varrho$  is a positive constant and  $\|x^{(4)}(t)\|_\infty$  is bounded by  $M$ , where  $M$  is a positive value. The truncation error associated with relation (2.2) is limited by the following inequality:

$$AE_r = \left\| \mathcal{J}_{0,t_r}^\varrho [x(t)] - (\mathcal{J}_{0,t_r}^\varrho [x(t)])_{approx} \right\|_\infty \leq \frac{Mr^\varrho}{16 \times 4! \Gamma(\varrho + 1)} \delta^{\varrho+4}. \tag{2.5}$$

*Proof.* Define  $S_m(t)$  as an interpolation function, which approximates  $x(t)$  within the subinterval  $[t_m, t_{m+1}] \subseteq \Phi$ , where  $m = 0, 1, \dots, r - 1$ . Consequently, for any chosen value  $\mu_m \in (t_m, t_{m+1})$ , it follows that:

$$\mathcal{E}_m(t) := x_m(t) - S_m(t) = (t - t_m)^2 (t - t_{m+1})^2 \frac{x^4(\mu_m)}{4!},$$

therefore,

$$\begin{aligned} \left\| \mathcal{J}_{0,t_r}^\varrho [x(t)] - (\mathcal{J}_{0,t_r}^\varrho [x(t)])_{approx} \right\|_\infty &= \frac{1}{\Gamma(\varrho)} \int_0^{t_r} \|(t_r - \varsigma)^{\varrho-1} \mathcal{E}(\varsigma)\|_\infty d\varsigma \\ &= \frac{1}{\Gamma(\varrho)} \sum_{m=0}^{r-1} \int_{t_m}^{t_{m+1}} (t_r - \varsigma)^{\varrho-1} \left\| (t - t_m)^2 (t - t_{m+1})^2 \frac{x^4(\mu_m)}{4!} \right\|_\infty d\varsigma \\ &= \frac{t_r^\varrho M}{16 \times 4! \Gamma(\varrho + 1)} \delta^4 = \frac{r^\varrho M}{16 \times 4! \Gamma(\varrho + 1)} \delta^{\varrho+4}. \end{aligned}$$

□



**Proposition 2.2.** According to the conditions outlined in Proposition 2.1, it is possible to express the numerical solution of the FIDE (1.1) in the following manner:

$$\begin{aligned}
 x_r &= x_0 + \sum_{i=1}^{\nu} \Upsilon_i(x_i) + \frac{\delta^\varrho}{\Gamma(\varrho+4)} \left( 6(\varrho+1)\Psi(t_r, x_r^p) - 2\varrho\delta\Psi'(t_r, x_r^p) \right) \\
 &+ \sum_{m=0}^{r-1} \frac{\delta^\varrho}{\Gamma(\varrho+4)} \left( \alpha_{m,r}\Psi(t_m, x_m) + \delta\beta_{m,r}\Psi'(t_m, x_m) \right),
 \end{aligned} \tag{2.6}$$

where  $\alpha_{m,r}$  and  $\beta_{m,r}$  are defined in (2.3) and (2.4).

*Proof.* Upon integration, the FIDE (1.1) can now be expressed as follows:

$$x(t) = \begin{cases} x_0 + \int_0^t \frac{(t-\varsigma)^{\varrho-1}}{\Gamma(\varrho)} \cdot \Psi(\varsigma, x(\varsigma))d\varsigma, & \text{for } t \in [0, t_1], \\ x_0 + \Upsilon_1(x_1) + \int_0^t \frac{(t-\varsigma)^{\varrho-1}}{\Gamma(\varrho)} \cdot \Psi(\varsigma, x(\varsigma))d\varsigma, & \text{for } t \in (t_1, t_2], \\ \vdots & \vdots \\ x_0 + \sum_{i=1}^{\nu} \Upsilon_i(x_i) + \int_0^t \frac{(t-\varsigma)^{\varrho-1}}{\Gamma(\varrho)} \cdot \Psi(\varsigma, x(\varsigma))d\varsigma, & \text{for } t \in (t_\nu, T], \end{cases} \tag{2.7}$$

or

$$x(t) = x_0 + \sum_{i=1}^{\nu} \Upsilon_i(x_i) + \mathcal{J}_{0,t}^\varrho \Psi(t, x(t)), \quad \nu = 1, 2, \dots, u. \tag{2.8}$$

Applying the formula expressed in Equation (2.2), we obtain the following result:

$$x_r = x_0 + \sum_{i=1}^{\nu} \Upsilon_i(x_i) + \sum_{m=0}^r \frac{\delta^\varrho}{\Gamma(\varrho+4)} \left( \alpha_{m,r}\Psi(t_m, x_m) + \delta\beta_{m,r}\Psi'(t_m, x_m) \right), \tag{2.9}$$

where  $\alpha_{m,r}$  and  $\beta_{m,r}$  are defined in (2.3) and (2.4), respectively. Since  $x_r$  appears on both sides of Equation (2.9), we employ a predicted value approach as outlined below:

$$x_r^p = x_0 + \frac{\delta^\varrho}{\Gamma(\varrho+1)} \sum_{m=0}^{r-1} \left( (r-m)^\varrho - (r-m-1)^\varrho \right) \Psi(t_m, x_m). \tag{2.10}$$

Therefore, we obtain:

$$\begin{aligned}
 x_r &= x_0 + \sum_{i=1}^{\nu} \Upsilon_i(x_i) + \frac{\delta^\varrho}{\Gamma(\varrho+4)} \left( \alpha_{r,r}\Psi(t_r, x_r^p) + \delta\beta_{r,r}\Psi'(t_r, x_r^p) \right) \\
 &+ \sum_{m=0}^{r-1} \frac{\delta^\varrho}{\Gamma(\varrho+4)} \left( \alpha_{m,r}\Psi(t_m, x_m) + \delta\beta_{m,r}\Psi'(t_m, x_m) \right).
 \end{aligned} \tag{2.11}$$

Since  $\alpha_{r,r} = 6(\varrho+1)$  and  $\beta_{r,r} = -2\varrho$ , we have:

$$\begin{aligned}
 x_r &= x_0 + \sum_{i=1}^{\nu} \Upsilon_i(x_i) + \frac{\delta^\varrho}{\Gamma(\varrho+4)} \left( 6(\varrho+1)\Psi(t_r, x_r^p) - 2\varrho\delta\Psi'(t_r, x_r^p) \right) \\
 &+ \sum_{m=0}^{r-1} \frac{\delta^\varrho}{\Gamma(\varrho+4)} \left( \alpha_{m,r}\Psi(t_m, x_m) + \delta\beta_{m,r}\Psi'(t_m, x_m) \right).
 \end{aligned} \tag{2.12}$$

□



TABLE 1. The comparison of  $\mathcal{E}_r$ ,  $ECO$ , and runtime (in seconds) for the Equation (3.3) using the SQ-algorithm [31] and the proposed approach, considering  $\varrho \in (0, 2)$  and  $\delta = \{0.02, 0.01, 0.005\}$  over the interval  $t \in [0, 3.5]$ .

$\varrho$	$\delta$	SQ-algorithm [31]			Proposed approach		
		$\mathcal{E}_r$	$ECO$	$Runtime$	$\mathcal{E}_r$	$ECO$	$Runtime$
0.4	0.02	$2.87 \times 10^{-4}$	2.085	5.825	$5.09 \times 10^{-9}$	4.882	4.296
	0.01	$5.24 \times 10^{-5}$	2.140	21.672	$3.34 \times 10^{-10}$	4.737	15.735
	0.005	$1.02 \times 10^{-5}$	2.171	86.812	$2.85 \times 10^{-11}$	4.585	61.890
0.9	0.02	$3.15 \times 10^{-4}$	2.061	5.656	$5.60 \times 10^{-9}$	4.856	4.812
	0.01	$5.75 \times 10^{-5}$	2.120	21.672	$3.58 \times 10^{-10}$	4.727	15.079
	0.005	$4.88 \times 10^{-6}$	2.309	87.312	$1.77 \times 10^{-11}$	4.675	61.734
1.4	0.02	$1.87 \times 10^{-4}$	2.194	6.500	$4.49 \times 10^{-9}$	4.913	4.156
	0.01	$4.81 \times 10^{-5}$	2.158	22.906	$2.71 \times 10^{-10}$	4.785	15.359
	0.005	$6.50 \times 10^{-6}$	2254	88.734	$1.86 \times 10^{-11}$	4.665	62.656
1.9	0.02	$1.07 \times 10^{-4}$	2.336	5.844	$3.21 \times 10^{-9}$	5.000	4.140
	0.01	$3.81 \times 10^{-5}$	2.210	22.406	$1.87 \times 10^{-10}$	4.863	15.407
	0.005	$6.83 \times 10^{-5}$	2.245	85.812	$3.96 \times 10^{-12}$	4.956	61.375

### 3. ILLUSTRATIVE EXAMPLES

In this segment, we assess the precision and computational speed of the newly devised method. To quantify the accuracy, we consider the mean absolute error (MAE) denoted by  $\mathcal{E}_M$ , and the convergence order ( $ECO$ ). The mean absolute error ( $\mathcal{E}_r$ ) is calculated as the sum of the absolute errors over all intervals, divided by the total number of intervals  $r$ , expressed by the equation:

$$\mathcal{E}_r = \sum_{m=1}^r \frac{AE_m}{r}, \quad (3.1)$$

where  $AE_m$  is defined in (2.5), and  $M$  represents the count of interior mesh points. Furthermore, we determine the convergence order ( $ECO$ ) as the logarithm, with base  $\delta$ , of the mean absolute error  $\mathcal{E}_r$ , expressed by:

$$ECO = \log_{\delta}(\mathcal{E}_r). \quad (3.2)$$

These metrics provide insights into both the precision and the rate of convergence of the numerical solution. All computational experiments are conducted using Matlab v2019a, executed on an Intel (R) Core (TM) i3-8145U CPU @ 2.30 GHz machine. Furthermore, we compare our results with those obtained using the SQ-algorithm [31], providing a comprehensive evaluation of our proposed approach.

**Example 3.1.** Consider the following fractional integral of the function  $t^3 \sin(t)$ :

$$\mathcal{J}_{0,t}^{\varrho} \left( t^3 \sin(t) \right) = \frac{24t^{e+4}}{\Gamma(5+\varrho)} {}_2F_3 \left( [2.5, 3]; [1.5, 3+0.5\varrho, 2.5+0.5\varrho]; -0.25t^2 \right), \quad (3.3)$$

where  $\varrho > 0$  and the generalized hypergeometric function is defined as  ${}_sF_v(b_1, \dots, b_s; a_1, \dots, a_v; t)$  [31]. This expression provides a representation of the fractional integral of the given function, facilitating further analysis of its properties and behavior under fractional differentiation.

Our proposed approach's efficacy is showcased using the function  $\mathcal{J}_{0,t}^{\varrho}(t^3 \sin(t))$  as demonstrated in Example 3.1. Table 1 presents significant performance indicators, including  $\mathcal{E}_r$ ,  $ECO$ , and computational times (in seconds), for (3.3) across various  $\delta$  and  $\varrho \in (0, 2)$  settings over  $t \in [0, 3.5]$ . Remarkably, all findings exhibit enhancements compared to the SQ-algorithm baseline [31].



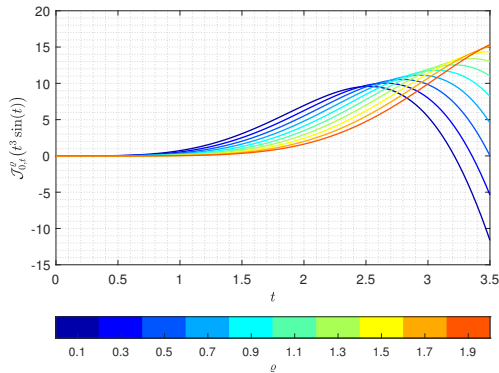


FIGURE 1. The impact of  $\rho$  on the dynamics of  $\mathcal{J}_{0,t}^\rho(t^3 \sin(t))$  using the Proposed Approach with  $\delta = 0.01$ .

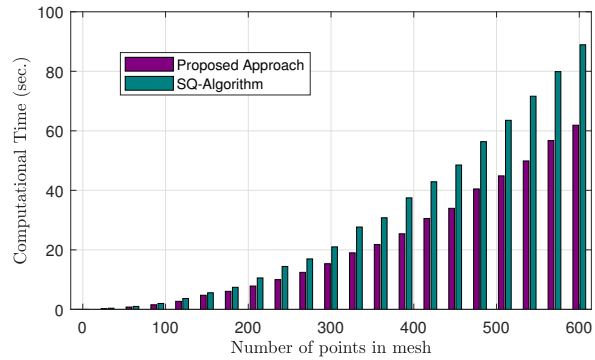


FIGURE 2. Comparative computational times of Proposed Approach and SQ-Algorithm [31] across mesh resolutions with  $\rho = 0.95$ .

These outcomes are further elucidated in Figures 1 and 2. As depicted in Figure 2, our proposed approach consistently outperforms the SQ-algorithm in computational efficiency.

Figure 1 illustrates the behavior of the expression  $\mathcal{J}_{0,t}^\rho(t^3 \sin(t))$  across a range of  $\rho$  values. Each curve represents a distinct  $\rho$  value, facilitating straightforward comparison. The colormap enhances clarity by highlighting the progression of  $\rho$  values, while the accompanying colorbar aids in associating colors with their respective  $\rho$  values, ensuring clear interpretation.

Furthermore, the bar plot in Figure 2 visually compares computational times between our Proposed Approach and the SQ-Algorithm across various mesh resolutions. Notably, our approach consistently demonstrates superior computational efficiency, emphasizing its optimization of computational resources and expeditious solution approximations in mathematical models.

**3.1. Application: Chaotic financial impulsive system.** The Lorenz system, introduced by Lorenz in 1963 to study convective atmospheric flow, has become a cornerstone in various scientific investigations. Initially devised to model the Earth’s atmosphere, where heat is applied from the bottom and dissipated from the top [22], this system has found widespread applications across diverse domains. It has been employed to explore phenomena ranging from economic dynamics [24] to chemical reactions [46], disk dynamos [11], and air pollution dynamics [4], among others.

Moreover, researchers have extensively studied the impact of impulsive perturbations on the Lorenz system, both in non-fractional and fractional contexts [1, 24, 49]. These investigations have provided valuable insights into the system’s behavior under sudden disturbances.

In this subsection, we focus specifically on the fractional impulsive Lorenz system, conceptualizing it as a fractional chaotic financial impulsive system. Our aim is to not only explore its dynamics but also to present numerical solutions that can enhance our understanding and facilitate further analysis of its complex behavior in financial contexts. Through these efforts, we aim to contribute to the growing body of knowledge surrounding impulsive systems and their applications in financial modeling and analysis.

The fractional chaotic financial system (FCFS) is described by the following equations:

$$\begin{cases} {}^C \mathcal{D}_{0,t}^{\alpha_1} x_1(t) = (25\phi + 10)(x_2(t) - x_1(t)), \\ {}^C \mathcal{D}_{0,t}^{\alpha_2} x_2(t) = (28 - 35\phi)x_1(t) + (29\phi - 1)x_2(t) - x_1(t)x_3(t), \\ {}^C \mathcal{D}_{0,t}^{\alpha_3} x_3(t) = -\frac{(8+\phi)}{3}x_3(t) + x_1(t)x_2(t), \\ x_1(0) = x_{1,0}, \quad x_2(0) = x_{2,0}, \quad x_3(0) = x_{3,0}, \end{cases} \tag{3.4}$$



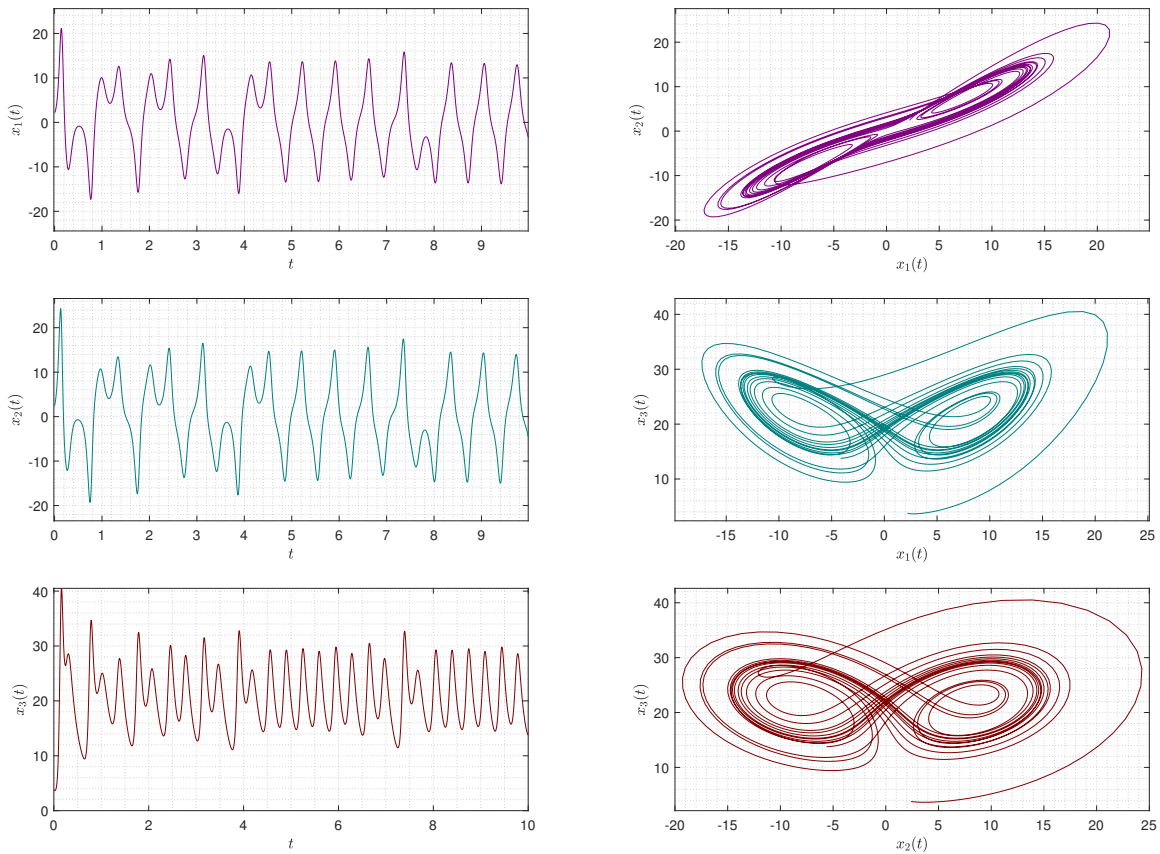


FIGURE 3. Time responses and phase curves of the FCFS from the proposed approach, with  $\phi = 1$ ,  $\varrho_1 = 0.93$ ,  $\varrho_2 = 0.98$ ,  $\varrho_3 = 0.85$ ,  $T = 10$ , and  $\delta = 0.005$ .

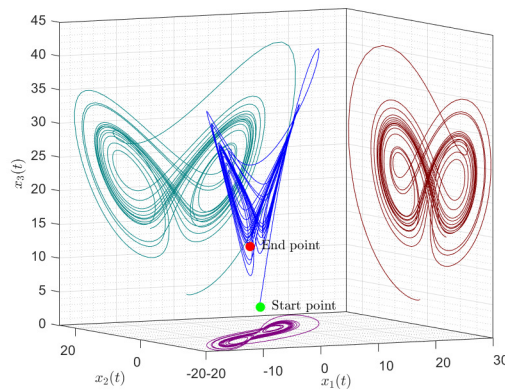


FIGURE 4. The 3D Trajectory of FCFS Attractor with Shadow Projections on Planes.

where  $\varrho_1, \varrho_2, \varrho_3 \in [0, 1]$  and  $\phi \in [0, 1]$ . This system includes several renowned systems, such as the Lorenz system for  $\phi = 0$  and the Chen system for  $\phi = 1$ .





In Figure 3, we illustrate the time responses and phase curves of the system described by Eq. (3.4), employing our proposed approach with initial conditions  $(x_{1,0}, x_{2,0}, x_{3,0}) = (2.2, 2.4, 3.8)$ ,  $T = 10$ , and  $\delta = 0.005$  for  $\phi = 1$  (Chen system). The plots are generated for specific values of  $\varrho_1 = 0.93$ ,  $\varrho_2 = 0.98$ , and  $\varrho_3 = 0.85$ . Analyzing these plots across various parameter combinations offers insights into the system's behavior under different conditions. Notably, the phase solutions of this system exhibit chaotic behaviors, as depicted in the figures. In addition, Figure 4 illustrates the 3D trajectory of the FCFS Attractor along with shadow projections on planes. This visualization provides further insights into the dynamic behavior of the system, allowing for a comprehensive understanding of its complex dynamics and attractor characteristics.

Furthermore, leveraging the concept of impulsivity, we can reformulate the FCFS (3.4) into the following system:

$$\begin{cases} {}^C \mathcal{D}_{0,t}^\varrho y(t) = Ay(t) + \Xi(t), \\ y(0) = y_0, \end{cases} \tag{3.5}$$

where  $\varrho = (\varrho_1, \varrho_2, \varrho_3)$ ,  $y(t) = [x_1(t), x_2(t), x_3(t)]^T$ ,

$$A = \begin{bmatrix} -(25\phi + 10) & 25\phi + 10 & 0 \\ 28 - 35\phi & 29\phi - 1 & 0 \\ 0 & 0 & -\frac{8+\phi}{3} \end{bmatrix},$$

and

$$\Xi(t) = \begin{bmatrix} 0 \\ -x_1(t)x_3(t) \\ x_1(t)x_2(t) \end{bmatrix}.$$

Hence, the fractional impulsive control of the (3.5) is described as

$$\begin{cases} {}^C \mathcal{D}_{0,t}^\varrho y(t) = Ay(t) + \Xi(t), & t \in \Phi' := \Phi \setminus \{t_1, t_2, \dots, t_u\}, \\ \Delta y(t) = y(t_\nu^+) - y(t_\nu^-) = \Upsilon_\nu(y(t_\nu)), & \nu = 1, 2, \dots, u, \\ y(0^+) = y_0, \end{cases} \tag{3.6}$$

where  $z_0 = (x_{1,0}, x_{2,0}, x_{3,0}) = (2.2, 2.4, 3.8)$ . This formulation allows for a deeper exploration of the system's dynamics under varying conditions, particularly through the application of fractional impulsive control techniques.

To explore the effects of selecting various impulses, we examine a specific scenario where the matrix  $C_\nu$  is given by:

$$C_\nu = \begin{bmatrix} -0.58 & 0 & 0 \\ 0 & -0.68 & 0 \\ 0 & 0 & -0.78 \end{bmatrix}.$$

The impact of various impulses is illustrated in Figure 5. Here, we present the numerical solutions of system (3.6) using the proposed approach, incorporating the matrix  $C_\nu$ , over the interval  $t \in [0, 2]$ . The simulations are conducted with parameter values  $\varrho_1 = 0.93$ ,  $\varrho_2 = 0.98$ , and  $\varrho_3 = 0.85$ , with a step size of  $\delta = 0.005$ . Notably, we examine different values for the impulsive interval  $\omega$ , including  $\{8^{-1}, 9^{-1}, 10^{-1}, 20^{-1}, 25^{-1}, 30^{-1}\}$ . These variations in the impulsive interval provide insights into how the system's behavior is affected by different impulsive stimuli.

#### 4. CONCLUSION

This study delved into an explicit approximation method for computing solutions to fractional systems with impulsive effects. The algorithm employed cubic spline interpolation for fractional-order integral operators and fractional impulsive differential equations. A comparative analysis was conducted with another algorithm, with results presented through figures and tables, focusing on mean absolute error, experimental convergence order, and computational runtime. Additionally, the proposed approach was applied to analyze a fractional chaotic financial system, a subset of the Lorenz system family often employed in financial modeling. Various impulsive intervals were examined to assess the effects of impulsive behaviors on this system. Furthermore, the impact of selecting different impulses was investigated. It is important to note that future research endeavors could explore the application of the proposed algorithm in solving other fractional systems with impulsive effects.





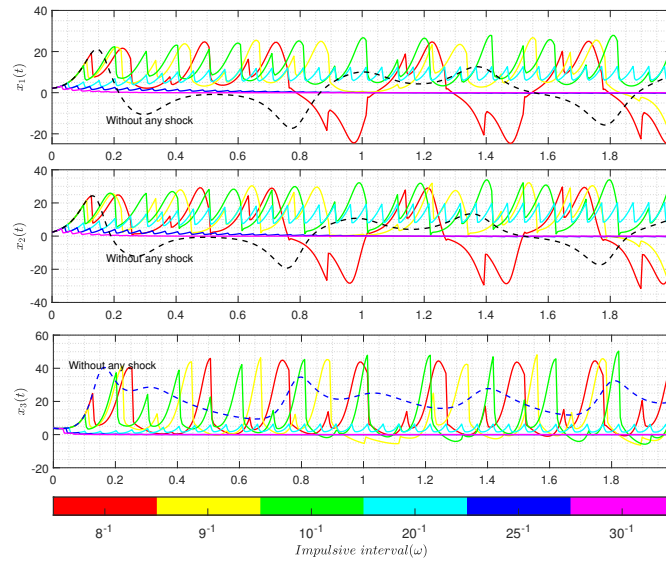


FIGURE 5. The Numerical computation of fractional impulsive system results employ the proposed approach across various impulsive intervals, with  $\varrho_1 = 0.93$ ,  $\varrho_2 = 0.98$ ,  $\varrho_3 = 0.85$ , and  $\delta = 0.005$ .

#### ACKNOWLEDGMENT

We would like to express our deep appreciation to the esteemed reviewers and the diligent editorial team for their thorough evaluation, valuable insights, and constructive suggestions on our manuscript.

#### REFERENCES

- [1] S. Aly, A. Al-Qahtani, H. B. Khenous, and G. M. Mahmoud, *Impulsive Control and Synchronization of Complex Lorenz Systems*, Abstract and Applied Analysis, *2014* (2014), 1–9.
- [2] A. Babaei and S. Banihashemi, *Reconstructing unknown nonlinear boundary conditions in a time-fractional inverse reaction-diffusion-convection problem*, Numerical Methods for Partial Differential Equations, *35*(3) (2019), 976–992.
- [3] S. Banihashemi, H. Jafari, and A. Babaei, *A novel collocation approach to solve a nonlinear stochastic differential equation of fractional order involving a constant delay*, Discrete and Continuous Dynamical Systems - Series S, *10* (2020).
- [4] A. H. Bukhari, M. A. Z. Raja, M. Shoaib, and A. K. Kiani, *Fractional order Lorenz based physics informed SARFIMA-NARX model to monitor and mitigate megacities air pollution*, Chaos, Solitons and Fractals, *161* (2022), 112375.
- [5] M. Caputo, *Linear models of dissipation whose Q is almost frequency independent-II*, Geophysical Journal International, *13*(5) (1967), 529–539.
- [6] M. Caputo, *Elasticit e dissipazione*, Zanichelli, Bologna, Italy, 1969.
- [7] J. Chen and M. Jiang, *Stability of Memristor-based Fractional-order Neural Networks with Mixed Time-delay and Impulsive*, Neural Processing Letters, *2022* (2022).
- [8] C. Djuikem, F. Grogard, and S. Touzeau, *Impulsive modelling of rust dynamics and predator releases for bio-control*, Mathematical Biosciences, *356* (2023), 108968.
- [9] A. Faghieh and P. Mokhtary, *A new fractional collocation method for a system of multi-order fractional differential equations with variable coefficients*, Journal of Computational and Applied Mathematics, *383* (2021), 113139.



- [10] T. A. Faree and S. K. Panchal, *Existence of solution for impulsive fractional differential equations with nonlocal conditions by topological degree theory*, Results in Applied Mathematics, 18 (2023), 100377.
- [11] C. Feng, L. Li, Y. Liu, and Z. Wei, *Global Dynamics of the Chaotic Disk Dynamo System Driven by Noise*, Complexity, 2020 (2020), 1–9.
- [12] J. Fu, M. Yu, and T.-D. Ma, *Modified impulsive synchronization of fractional order hyperchaotic systems*, Chinese Physics B, 20(12) (2011).
- [13] F. Ghanbari, K. Ghanbari, and P. Mokhtary, *Generalized JacobiGalerkin method for nonlinear fractional differential algebraic equations*, Computational and Applied Mathematics, 37(4) (2018), 5456–5475.
- [14] F. Gholami Bahador, P. Mokhtary, and M. Lakestani, *Mixed Poisson-Gaussian noise reduction using a time-space fractional differential equations*, Information Sciences, 647 (2023), 119417.
- [15] C. Ionescu, A. Lopes, D. Copot, J. A. T. Machado, and J. H. T. Bates, *The role of fractional calculus in modeling biological phenomena: A review*, Communications in Nonlinear Science and Numerical Simulation, 51 (2017), 141–159.
- [16] B. Jalili, P. Jalili, A. Shateri, and D. Domiri Ganji, *Rigid plate submerged in a Newtonian fluid and fractional differential equation problems via Caputo fractional derivative*, Partial Differential Equations in Applied Mathematics, 6 (2022), 100452.
- [17] W. Jung and J. H. Lee, *Quantile Impulse Response Analysis with Applications in Macroeconomics and Finance*, in *Essays in Honor of Joon Y. Park: Econometric Methodology in Empirical Applications*, Emerald Publishing Limited, (2023), 99–131.
- [18] R. Karimi, A. Dabiri, J. Cheng, and E. A. Butcher, *Probabilistic-Robust Optimal Control for Uncertain Linear Time-delay Systems by State Feedback Controllers with Memory*, 2018 Annual American Control Conference (ACC), 2018.
- [19] A. Kumar, R. K. Vats, A. Kumar, and D. N. Chalishajar, *Numerical approach to the controllability of fractional order impulsive differential equations*, Demonstratio Mathematica, 53(1) (2020), 193–207.
- [20] X. Li and S. Song, *Impulsive Systems with Delays*, Springer Singapore, 2022.
- [21] Z. Li, L. Chen, and Z. Liu, *Periodic solution of a chemostat model with variable yield and impulsive state feedback control*, Applied Mathematical Modelling, 36(3) (2012), 1255–1266.
- [22] E. N. Lorenz, *Deterministic Nonperiodic Flow*, Journal of the Atmospheric Sciences, 20(2) (1963), 130–141.
- [23] Y. Guan, Z. Zhao, and X. Lin, *On the existence of solutions for impulsive fractional differential equations*, Advances in Mathematical Physics, 2017 (2017).
- [24] R. Ma, J. Wu, K. Wu, and X. Pan, *Adaptive fixed-time synchronization of Lorenz systems with application in chaotic finance systems*, Nonlinear Dynamics, 109(4) (2022), 3145–3156.
- [25] A. Martynyuk, G. Stamo, I. Stamo, and E. Gospodinova, *Formulation of Impulsive Ecological Systems Using the Conformable Calculus Approach: Qualitative Analysis*, Mathematics, 11(10) (2023), 2221.
- [26] L. Mei, H. Sun, and Y. Lin, *Numerical method and convergence order for second-order impulsive differential equations*, Advances in Difference Equations, 2019(1) (2019).
- [27] B. P. Moghaddam, Z. S. Mostaghim, A. A. Pantelous, and J. A. Tenreiro Machado, *An integro quadratic spline-based scheme for solving nonlinear fractional stochastic differential equations with constant time delay*, Communications in Nonlinear Science and Numerical Simulation, 92 (2021), 105475.
- [28] B. P. Moghaddam, M. Pishbin, Z. S. Mostaghim, O. S. Iyiola, A. Galhano, and A. M. Lopes, *A Numerical Algorithm for Solving Nonlocal Nonlinear Stochastic Delayed Systems with Variable-Order Fractional Brownian Noise*, Fractal and Fractional, 7(4) (2023), 293.
- [29] Z. Moniri, B. P. Moghaddam, and M. Zamani Roudbaraki, *An Efficient and Robust Numerical Solver for Impulsive Control of Fractional Chaotic Systems*, Journal of Function Spaces, 2023 (2023), 1–10.
- [30] Z. S. Mostaghim, B. P. Moghaddam, and H. S. Haghgozar, *Computational technique for simulating variable-order fractional Heston model with application in US stock market*, Mathematical Sciences, 12(4) (2018), 277–283.
- [31] Z. S. Mostaghim, B. P. Moghaddam, and H. S. Haghgozar, *Numerical simulation of fractional-order dynamical systems in noisy environments*, Computational and Applied Mathematics, 37(5) (2018), 6433–6447.



- [32] G. Narayanan, M. S. Ali, R. Karthikeyan, G. Rajchakit, and A. Jirawattanapanit, *Impulsive control strategies of mRNA and protein dynamics on fractional-order genetic regulatory networks with actuator saturation and its oscillations in repressilator model*, Biomedical Signal Processing and Control, 82 (2023), 104576.
- [33] N. Nyamoradi, *Existence of solutions for a class of second-order differential equations with impulsive effects*, Mathematical Methods in the Applied Sciences, 38(18) (2015), 5023–5033.
- [34] Z. Odibat, V. S. Erturk, P. Kumar, A. B. Makhlof, and V. Govindaraj, *An Implementation of the Generalized Differential Transform Scheme for Simulating Impulsive Fractional Differential Equations*, Mathematical Problems in Engineering, 2022 (2022), 1–11.
- [35] B. P. Moghaddam, A. Dabiri, Z. S. Mostaghim, and Z. Moniri, *Numerical solution of fractional dynamical systems with impulsive effects*, International Journal of Modern Physics C, 34(01) (2023).
- [36] B. P. Moghaddam, A. Dabiri, and J. A. T. Machado, *Application of variable-order fractional calculus in solid mechanics*, in D. Bleanu and A. Mendes Lopes (eds.), Applications in Engineering, Life and Social Sciences, Part A, De Gruyter, 2019, 207–224.
- [37] X. J. Ran, M. Z. Liu, and Q. Y. Zhu, *Numerical methods for impulsive differential equation*, Mathematical and Computer Modelling, 48(1-2) (2008), 46–55.
- [38] D. Raghavan and S. Nagarajan, *Convergence on iterative learning control of Hilfer fractional impulsive evolution equations*, Asian Journal of Control, 25(3) (2022), 2183–2193.
- [39] S. G. Samko, A. A. Kilbas, and O. I. Marichev, *Fractional Integrals and Derivatives: Theory and Applications*, Gordon and Breach Science Publishers, 1993.
- [40] A. Shahnazi-Pour, B. P. Moghaddam, and A. Babaei, *Numerical simulation of the Hurst index of solutions of fractional stochastic dynamical systems driven by fractional Brownian motion*, Journal of Computational and Applied Mathematics, 386 (2021), 113210.
- [41] I. Stamova and G. Stamov, *Applied Impulsive Mathematical Models*, Springer International Publishing, 2016.
- [42] G. Stamov and I. Stamova, *Extended Stability and Control Strategies for Impulsive and Fractional Neural Networks: A Review of the Recent Results*, Fractal and Fractional, 7(4) (2023), 289.
- [43] I. M. Stamova and A. G. Stamov, *Impulsive control on the asymptotic stability of the solutions of a Solow model with endogenous labor growth*, Journal of the Franklin Institute, 349(8) (2012), 2704–2716.
- [44] I. Stamova and J. Henderson, *Practical stability analysis of fractional-order impulsive control systems*, ISA Transactions, 64 (2016), 77–85.
- [45] Y. Talaei, S. Shahmorad, and P. Mokhtary, *A new recursive formulation of the Tau method for solving linear Abel-Volterra integral equations and its application to fractional differential equations*, Calcolo, 56(4) (2019), 1–20.
- [46] U. S. Thounaojam, *Stochastic chaos in chemical Lorenz system: Interplay of intrinsic noise and nonlinearity*, Chaos, Solitons and Fractals, 165 (2022), 112763.
- [47] Q. Wang and M. Wang, *Existence of solution for impulsive differential equations with indefinite linear part*, Applied Mathematics Letters, 51 (2016), 41–47.
- [48] G.-C. Wu, D. Q. Zeng, and D. Baleanu, *Fractional Impulsive Differential Equations: Exact Solutions, Integral Equations and Short Memory Case*, Fractional Calculus and Applied Analysis, 22(1) (2019), 180–192.
- [49] X. Wu, J. A. Lu, C. K. Tse, J. Wang, and J. Liu, *Impulsive control and synchronization of the Lorenz systems family*, Chaos, Solitons and Fractals, 31(3) (2007), 631–638.
- [50] X. Yang, *Existence and multiplicity of weak solutions for a nonlinear impulsive  $(q, p)$ -Laplacian dynamical system*, Advances in Difference Equations, 2017(1) (2017).
- [51] X. Zhang, D. Li, and X. Zhang, *Adaptive impulsive synchronization for a class of fractional order complex chaotic systems*, Journal of Vibration and Control, 25(10) (2019), 1614–1628.
- [52] Y. Zhao, C. Luo, and H. Chen, *Existence Results for Non-instantaneous Impulsive Nonlinear Fractional Differential Equation Via Variational Methods*, Bulletin of the Malaysian Mathematical Sciences Society, 43(3) (2019), 2151–2169.

